ADVANCED MATERIALS

[30] a) D. Qin, Y. Xia, H. Yang, C. Zhu, G. M. Whitesides, *Adv. Mater.* **1999**, *11*, 1433. b) B. Messer, J. H. Song, P. Yang, *J. Am. Chem. Soc.* **2000**, *122*, 10 232.
[31] J. A. Massey, M. A. Winnik, I. Manners, V. Z.-H. Chan, J. M. Ostermann, R. Enchelmaier, J. P. Spatz, M. Möller, *J. Am. Chem. Soc.* **2001**, *123*, 3147.

Exchange Coupling and Remanence Enhancement in Nanocomposite Multilayer Magnets**

By *Wei Liu*, *Zhi-dong Zhang*,* *Jia-ping Liu*, *Li-jun Chen*, *Lian-long He*, *Yi Liu*, *Xiao-kai Sun*, and *David J. Sellmyer*

After experimental evidence of intergrain exchange coupling was reported,[1] nanocomposite magnets with high remanence and large energy products were predicted.[2,3] However, the experimental values of the maximum magnetic energy product of nanocomposite bulk magnets have been much lower than the theoretically predicted ones. We report on the exchange coupling and remanence enhancement in nanocomposite $(Nd,Dy)(Fe,Co,Nb,B)_{5.5}$/α-Fe thin films prepared by sputtering and heat treatments. The coercivity of a single Ti-buffered $(Nd,Dy)(Fe,Co,Nb,B)_{5.5}$ layer is as large as 1.85 T, while a high remanence of $J_r = 1.31$ T and a high maximum-energy product of $(BH)_{max} = 203$ kJ m^{-3} are achieved in the nanocomposite multilayer films. Well-designed multilayer films consist of a magnetically hard $Nd_2Fe_{14}B$-type phase with a grain size of 40 nm, and a magnetically soft α-Fe phase, which forms a continuous layer. Our results suggest that nanocomposite multilayer films with well-distributed fine grains of the hard and soft magnetic phases could constitute a new generation of permanent-magnet materials.

Based on the theoretical explanation of the exchange coupling,[2–4] it was expected that the next generation of permanent magnets would be realized in nanocomposite magnets that combine large values of coercivity and magnetization of hard and soft magnetic phases, respectively. A high remanence and large maximum magnetic energy product would be obtained if the grains of the soft and hard phases could be coupled well in nanocomposite magnets, as predicted based on micromagnetic calculations.[2,3] Up to now, the energy products of nanocomposite magnets prepared by means of rapid quenching and mechanical alloying have been much lower than theoretically expected, because of difficulties in controlling the nanostructures in nanocomposite bulk magnets.[5–8]

Recently, some studies on exchange coupling were carried out by Sellmyer and co-workers for nanostructured CoSm/FeCo and PrCo/Co multilayer systems prepared by sputtering and subsequent heat treatment.[9,10] Magnetic properties of exchange-coupled α-Fe/Nd–Fe–B multilayer magnets were investigated by Shindo and Ishizone,[11] and the observations for Nd–Fe–B/Fe/Nd–Fe–B trilayer films were reported by Parhofer et al.[12,13] and Yang and Kim.[14] Generally, in contrast to bulk magnets, the structure of the multilayer materials can be easily controlled during the preparation process by properly arranging different layers, adjusting the thickness of the layers of the soft and hard phases, and annealing at the proper temperatures. This leads to an optimized average grain size and grain-size distribution. Thus, it is possible to form a nearly ideal nanocomposite structure. Here, we report on the structural and magnetic properties of nanocomposite $(Nd,Dy)(Fe,Co,Nb,B)_{5.5}$/α-Fe multilayer magnets synthesized by sputtering and subsequent annealing. The high-performance multilayer magnets are also potentially useful for certain modern applications, where magnets need to be as small as possible.

Prior to studying the structural and magnetic properties of multilayers, we investigated a single hard-phase layer, Ti(10 nm)/NdDyFeCoNbB(240 nm)/Ti(10 nm)/(Si substrate). As was found also in Nd–Fe–B thin films reported by Jiang and O'Shea,[15] the as-deposited Ti-buffered single-layer hard-phase thin film on the Si substrate is amorphous. After annealing at 550 °C for 30 min, a magnetically hard phase of $Nd_2Fe_{14}B$-type is formed in the film. The magnetic measurement along the direction parallel to the film surface indicates that the highest value achieved for intrinsic coercivity at room temperature is 1473 kA m^{-1} (1.85 T).

Figure 1 shows a transmission electron microscopy (TEM) bright-field image of the as-deposited Ti(10 nm)/[NdDyFeCoNbB(16 nm)Fe(6 nm)] × 20/Ti(10 nm)/(glass-ceramics substrate) multilayer thin film. The inset shows a high-resolution TEM image. The cross-sectional view shows that the distribution of the soft- and hard-phase layers is very uniform. Selected-area electron diffraction analyses reveal that the wide NdDyFeCoNbB layer is amorphous, and the narrow one corresponds to Fe. Clearly, the ratio and distribution of the soft and hard phases can be controlled well in this way.

For the NdDyFeCoNbB/α-Fe multilayers on glass-ceramics substrates, annealed at 575 °C for 30 min, the X-ray diffraction (XRD) analysis shows a large amount of α-Fe due to the

[*] Prof. Z.-d. Zhang, Prof. W. Liu[+], Prof. Z.-d. Zhang, L.-j. Chen, Prof. L.-l. He, Prof. X.-k. Sun
Shenyang National Laboratory for Materials Science
Institute of Metal Research, and International Center for Materials Physics, Chinese Academy of Sciences
Shenyang 110016 (PR China)
E-mail: zdzhang@imr.ac.cn
Prof. J.-p. Liu[++], Prof. Y. Liu[+++], Prof. D. J. Sellmyer
Department of Physics and Astronomy and Center for Materials Research and Analysis, University of Nebraska
Lincoln, NE 68588-0113 (USA)
[+] Second address: Department of Physics and Astronomy and Center for Materials Research and Analysis, University of Nebraska, Lincoln, NE 68588-0113, USA.
[++] Second address: Institute for Micromanufacturing, Louisiana Tech University, Ruston, LA 71272, USA.
[+++] Second address: Department of Mechanical Engineering, University of Michigan, Ann Arbor, MI 48109-2125, USA.
[**] This work is supported by the U.S. NSF under grant INT-9812082, DOE, AFOSR, and the National Natural Science Foundation of China under grant 59725103 and 50071062, the National 863 project under grant 2002AA302603 and the Science and Technology Commission of Shenyang. We also thank L. Gao and Prof. S. H. Liou for MFM observations.

  0935-9648/02/2412-1832 $ 17.50+.50/0 *Adv. Mater.* **2002**, *14*, No. 24, December 17

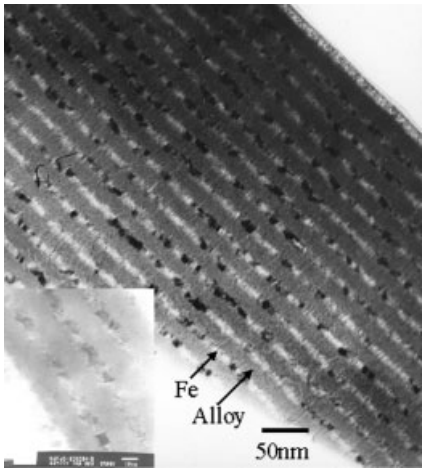

Fig. 1. TEM bright-field image of the as-deposited Ti(10 nm)/[NdDyFeCoNbB(16 nm)Fe(6 nm)] × 20/Ti(10 nm)/(glass-ceramics substrate) multilayer thin film. The inset is a high-resolution TEM image of this sample.

existence of Fe layers in the multilayer film. Almost all other XRD peaks of the films correspond to randomly oriented $Nd_2Fe_{14}B$-type phases. Hysteresis loops at room temperature for Ti(10 nm)/[NdDyFeCoNbB(16 nm)Fe(4.5 nm)] × 20/Ti(10 nm)/(glass-ceramics substrate) and Ti(10 nm)/[NdDyFeCoNbB-(320 nm)/Ti(10 nm)/(glass-ceramics substrate) films annealed at 575 °C for 30 min are given in Figure 2. Compared with the result of the single-layer film, remanence enhancement is observed in the multilayer films. The Ti(10 nm)/[NdDyFeCoNbB(16 nm)Fe(4.5 nm)] × 20/Ti(10 nm) (glass-ceramics substrate) multilayer film shows a high remanence of $J_r = 1.31$ T and a high maximum magnetic energy product of $(BH)_{max} = 203$ kJ m^{-3}. These values are much higher than those of the single layer ($J_r = 0.85$ T and $(BH)_{max} = 117$ kJ m^{-3}). The coercivity of the former ($_JH_c = 615$ kA m^{-1} (0.77 T) is little lower than that of the latter [$_JH_c = 832$ kA m^{-1} (1.05 T)]. The remanence ratio of the multilayers is 0.78. It is clear that the exchange coupling between the layers of soft and hard phases results in a significant enhancement of the remanence and an increase of the maximum magnetic energy product in this type of the nanocomposite magnet.

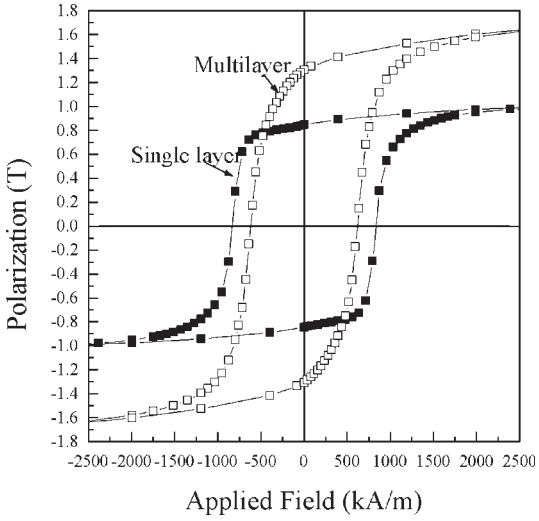

Fig. 2. Room temperature hysteresis loops for Ti(10 nm)Ti/[NdDyFeCoNbB-(16 nm)Fe(4.5 nm)] × 20/Ti(10 nm)/(glass-ceramics substrate) multilayer (□), and Ti(10 nm)Ti/[NdDyFeCoNbB(320 nm)/Ti(10 nm)/(glass-ceramics substrate) films annealed at 575 °C for 30 min (■).

To investigate the nanostructures of the multilayer magnets, a plan view was obtained by TEM examination. Electron diffraction confirmed that the hard magnetic phase has the $Nd_2Fe_{14}B$-type structure. Figures 3a and 3b show the plan-view elemental maps acquired by electron energy loss spectroscopy (EELS). The intensity (brightness) corresponds to the concentration of the elements concerned. Since only the hard phase contains Nd, the Nd map in Figure 3a reveals the grain morphology of the hard phase with a grain size of about 40 nm. In contrast, the Fe map in Figure 3b reveals the morphology of the soft phase, indicating that a α-Fe phase could appear as a continuous layer, in a good agreement with the results in Figure 1. Figure 3c shows a magnetic force microscopy (MFM) image of the same film. It shows a domain structure with characteristic lengths of about 300 nm. It is concluded that although the nanostructured soft and hard phases diffused into each other during annealing, the exchange-coupled soft and hard composite nanostructure still remains. The best magnetic properties are obtained for films annealed at 575 °C, while remanence enhancement is observed for those annealed at both 575 °C and 550 °C. A relatively low annealing temperature leads to decoupling, because the hard phase in the film is not formed completely. If the annealing temperature is too high, a decoupling effect is clearly observed, because of the continuous growth of α-Fe, which destroys the exchange coupling.

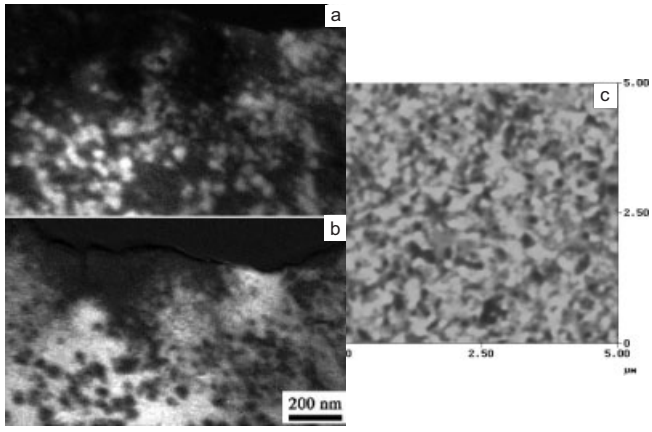

Fig. 3. a) EELS map of Nd, b) Fe, and c) MFM image of Ti(10 nm)/[NdDyFeCoNbB(16 nm)/Fe(4.5 nm)] × 20/Ti(10 nm)/(glass-ceramics substrate) multilayers annealed at 575 °C for 30 min.

In conclusion, we have succeeded in preparing the single-layer $Nd_2Fe_{14}B$-type hard phase and nanocomposite multilayers with a hard and α-Fe soft phase by sputtering and subsequent heat treatment. The nanostructures of the multilayers can be controlled well by preparing different layers and by adjusting the thickness of the layers for the soft and hard phases. After annealing at appropriate temperatures, the mutually dis-

  0935-9648/02/2412-1833 $ 17.50+.50/0

ADVANCED MATERIALS

persed soft and hard phases can be formed in the partial layers of the multilayer magnets, while the α-Fe phase appears also in the form of the continuous layer. The high-energy products achieved in this work show much promise in the application of nanocomposite multilayers as permanent magnet thin films.

Experimental

$(Nd,Dy)(Fe,Co,Nb,B)_{5.5}$/α-Fe thin films were prepared with a multiple-gun dc- and rf-sputtering system by depositing $(Nd_{0.9}Dy_{0.1})(Fe_{0.77}Co_{0.12}Nb_{0.03}B_{0.08})_{5.5}$ alloy and Fe targets onto glass-ceramics or silicon substrates, covered with a 10 or 20 nm Ti-buffer. The alloy target was homemade by sintering powdered ingots, and all other products were commercially sourced. The purity of every target was higher than 99.9 %. The base pressure of the sputtering system was $2–3 \times 10^{-7}$ Torr, and the Ar pressure during the sputtering was 5 mTorr. The thickness of the films was measured by weighing the films. The as-deposited films were then heat-treated in a furnace with a vacuum of 2×10^{-7} Torr. The crystalline structure of the phases in the films was determined by X-ray diffractometry with Cu Kα radiation, and by TEM. The magnetic domains were observed by MFM. Magnetic properties of the films were measured by an alternating gradient force magnetometer (AGFM) and a superconducting quantum interference device (SQUID) magnetometer. The in-plane hysteresis loops as well as the values for the magnetic properties were recorded without the demagnetizing-factor correction.

Received: August 20, 2002
Final version: October 8, 2002

[1] R. Coehoorn, D. B. de Mooji, C. D. E. Waard, *J. Magn. Magn. Mater.* **1989**, *80*, 101.
[2] R. Skomski, J. M. D. Coey, *Phys. Rev. B* **1993**, *48*, 15 812.
[3] T. Schrefl, J. Fidler, H. Kromüller, *Phys. Rev. B* **1994**, *49*, 6100.
[4] E. F. Kneller, R. Hawig, *IEEE Trans. Magn*. **1991**, 27, 3588.
[5] J. Ding, P. G. McCormick, R. Street, *J. Magn. Magn. Mater.* **1993**, *124*, 1.
[6] A. Manaf, R. A. Buckley, H. A. Davies, *J. Magn. Magn. Mater.* **1993**, *128*, 302.
[7] L. Withanawasam, G. C. Hadjipanayis, R. F. Krause, *J. Appl. Phys.* **1994**, *75*, 6646.
[8] X. K. Sun, J. Zhang, Y. L. Chu, W. Liu, B. Z. Cui, Z. D. Zhang, *Appl. Phys. Lett.* **1999**, *74*, 1740.
[9] I. A. Al-Omari, D. J. Sellmyer, *Phys. Rev. B* **1995**, *52*, 3441.
[10] J. P. Liu, Y. Liu, R. Skomski, D. J. Sellmyer, *IEEE Trans. Magn.* **1999**, *35*, 3241.
[11] M. Shindo, M. Ishizone, *J. Appl. Phys.* **1997**, *81*, 4444.
[12] S. Parhofer, J. Wecker, C. Kuhrt, G. Gieres, *IEEE Trans. Magn.* **1996**, *32*, 4437.
[13] S. Parhofer, G. Gieres, J. Wecker, L. Schultz, *J. Magn. Magn. Mater.* **1996**, *163*, 32.
[14] C. J. Yang, S. W. Kim, *J. Magn. Magn. Mater.* **1999**, *202*, 311.
[15] H. Jiang, M. J. O'Shea, *J. Magn. Magn. Mater.* **2000**, *212*, 59.

Triplet Formation In Polyfluorene Devices**

By *Anoop S. Dhoot* and *Neil C. Greenham**

Exciton formation in polymer light-emitting diodes (LEDs) occurs by recombination of electrons and holes injected from opposite electrodes. Excitons may be formed in either the singlet or triplet spin state, and usually only singlet excitons can undergo radiative decay. Formation of triplet states therefore represents an important loss mechanism that limits the efficiency of polymer LEDs. It has typically been assumed that exciton formation occurs on a statistical basis, leading to a singlet formation probability of only 25 %. However, recent measurements of LED efficiency have suggested that this limit is broken in conjugated polymers.[1,2] Indeed, through a detailed study of triplet absorptions in working LEDs, we have shown that 83 ± 7 % of excitons formed in a poly(*p*-phenylenevinylene) (PPV)-derivative LED are singlets rather than triplets.[3] Other experiments have also shown a deviation from the simple statistics model; magnetic resonance measurements have demonstrated spin-dependent exciton formation rates,[4,5] and electroluminescence measurements in platinum-containing polymers have measured a singlet formation probability of 57 %.[6]

In this paper, we study absorptions due to triplet excitons in technologically important polyfluorene LEDs using spectroscopic techniques, without the need to introduce phosphorescent materials to observe triplet emission. Although triplet excitons are not strongly coupled to the ground state, there is an allowed optical transition to a higher-lying triplet state. Measurement of this triplet absorption allows triplet populations to be quantified in a working device, and hence the ratio of singlet and triplet exciton formation can be estimated. We have studied triplet populations in a polyfluorene polymer, poly(9,9-dioctylfluorene) (F8), and copolymer, poly(9,9-dioctylfluorene-*co*-benzothiadiazole) (F8BT). Information about the triplet state in these polymers is currently limited, especially for F8BT. However, a detailed study of the photophysics of triplets in F8 was recently carried out by Cadby et al. using a combination of photoinduced absorption (PA) and magnetic resonance spectroscopy.[7,8] Their work identified and characterized absorptions due to triplets formed by intersystem crossing after photoexcitation in a pristine film. Here we show that triplets can be identified in F8 LEDs, and we then go on to calculate the singlet formation probability using methods developed previously for the study of infrared absorptions in PPV LEDs.[3] We also investigate the sub-gap absorptions present in F8BT single-polymer and blend devices, and find triplet behavior remarkably different to that seen in other devices.

Figure 1 shows the modulation spectrum of an F8 LED together with the PA spectrum at low temperatures. In the PA, we resolve a sharp feature at 1.51 eV, a broad absorption centered on 2.0 eV, and the onset of a small absorption at < 0.5 eV. These absorptions are consistent with the spectra of Cadby et al. We therefore assign the latter two absorptions to singly charged polarons, and the sharp feature at 1.51 eV to triplet excitons generated by intersystem crossing. In the device spectrum, three features at 0.84 eV, 1.55 eV, and 2.22 eV are clearly resolved. By analysis of the quadrature component of this spectrum, we can separate out overlapping species with different lifetimes. A distinct feature peaking at 1.55 eV emerges from such an analysis (Fig. 1, circles), which, al-

[*] Dr. N. C. Greenham, Dr. A. S. Dhoot
Cavendish Laboratory, University of Cambridge
Madingley Road, Cambridge CB3 0HE (UK)
E-mail: ncg11@cam.ac.uk

[**] This work was supported by the Engineering and Physical Sciences Research Council, United Kingdom, and by the European Commission IST Programme IST-2001-37375 (STEPLED).

